Cancer Center, Japan) between 1 August 2005, and 30 June 2010. Patients with incompletely resected tumours (R1 or R2) and those with multiple tumours or previous lung surgeries were not included in the database. The database has been maintained prospectively. The patient data obtained from this multicentre database were retrospectively analysed in the present study. High-resolution computed tomography (HRCT) and F-18-fluorodeoxyglucose positron emission tomography/computed tomography (FDG-PET/CT) followed by curative R0 resection were performed for all patients staged according to the tumour, node, metastasis (TNM) Classification of Malignant Tumours, 7th Edition [10]. Neither Mediastinoscopy nor endobronchial ultrasonography was routinely performed because all patients received preoperative HRCT and FDG-PET/CT. HRCT and FDG-PET revealed an absence of >1-cm enlargement in mediastinal or hilar lymph nodes and an absence of >1.5 accumulation for maximum standardized uptake values (SUVmax's) in these lymph nodes, respectively. Sublobar resection was allowed as an optional procedure for peripheral clinical T1N0M0 tumours that were intraoperatively assessed as N0 by frozen section evaluation of enlarged lymph nodes or by ensuring that there was no obvious lymph node enlargement in the thoracic cavity. Systematic lymph node dissection, such as that of hilar and mediastinal nodes, was performed during segmentectomy but not during wedge resection. All segmentectomies were performed exclusively in the patients who could tolerate lobectomy. All patients showing pathological lymph node metastasis received four cycles of platinum-based chemotherapy after surgery.

The inclusion criteria were preoperative staging determined using HRCT and FDG-PET/CT, curative surgery without neoadjuvant chemotherapy or radiotherapy and a definitive histopathological diagnosis of lung adenocarcinoma. This study was approved by the Institutional Review Boards (IRB) of the participating institutions (Hiroshima University Hospital IRB, No. EKI-644; Kanagawa Cancer Center IRB, No. KEN-31; Cancer Institute Hospital IRB, No. 2008-1018; Hyogo Cancer Center IRB, No. H20-RK-15). The requirement of informed consent from individual patients was waived because this study was a retrospective review of a patient database.

High-resolution computed tomography

Sixteen-row multidetector CT was used to obtain chest images, independent of subsequent FDG-PET/CT examinations. For high-resolution images of the tumours, the following parameters were used: 120 kVp, 200 mA, 1–2 mm section thickness, 512 × 512 pixel resolution, 0.5–1.0 s scanning time, a high-spatial reconstruction algorithm with a 20-cm field of view (FOV), and mediastinal (level, 40 HU; width, 400 HU) and lung (level, −600 HU; width, 1600 HU) window settings. GGO was defined as a misty increase in lung attenuation without obscuring the underlying vascular markings. Radiologically determined solid-dominant tumour was defined as a tumour with ≥50% solid component. Solid tumour size was defined as the maximum dimension of the solid component measured on lung window settings, excluding GGO [11]. Mixed GGO tumour was defined as a tumour that had both GGO and solid component. CT scans were reviewed and tumour sizes were determined by radiologists from each institution.

F-18-fluorodeoxyglucose positron emission tomography/computed tomography

The patients were instructed to fast for at least 4 h before intravenous injection of 74–370 MBq of FDG and were then advised to rest for at least 1 h before FDG-PET/CT scanning. Blood glucose levels were calculated before the tracer injection to confirm a level of <150 mg/dl [12]. Patients with blood glucose levels ≥150 mg/dl were excluded from the PET/CT imaging. For imaging, Discovery ST (GE Healthcare, Little Chalfont, UK), Aquiduo (Toshiba Medical Systems Corporation, Tochigi, Japan) or Biograph Sensation16 (Siemens Healthcare, Erlangen, Germany) integrated three-dimensional PET/CT scanner were used. Low-dose non-enhanced CT images of 2–4 mm section thickness for attenuation correction and localization of lesions identified by PET were obtained from the head to the pelvic floor of each patient according to a standard protocol.

Immediately after CT, PET was performed with the identical axial FOV for 2–4 min/table position, depending on the condition of the patient and the scanner performance. An iterative algorithm with CT-derived attenuation correction was used to reconstruct all PET images with a 50-cm FOV. An anthropomorphic body phantom (NEMA NU2-2001, Data Spectrum Corp, Hillsborough, NC, USA) was used to minimize the variations in SUVs among the institutions [13]. A calibration factor was derived by dividing the actual SUV by the gauged mean SUV in the phantom background to decrease interinstitutional SUV inconsistencies. The final SUV used in this study is referred to as the revised SUVmax [14]. The original SUVmax values were determined by radiologists from each institution.

Follow-up evaluation

All patients who underwent lung resection were followed up from the day of surgery. Postoperative follow-up procedures, including a physical examination, chest roentgenogram every 3 months and chest and abdominal CT examinations every 6 months, were performed for the first 2 years. Subsequently, a physical examination and chest roentgenogram were performed every 6 months, and a chest CT examination was performed every year.

Statistical analysis

Results are given as numbers (%) or medians, unless stated otherwise. A χ^2 test was used to compare categorical variable frequencies. Fisher's exact test was used when sample sizes were small. Mann–Whitney *U*-test was used to compare continuous variables. Recurrence-free survival (RFS) was defined as the time from the date of surgery until the first event (relapse or death due to any cause) or the last follow-up. The Kaplan–Meier method was used to assess RFS durations and these were compared using log-rank tests. To assess the potential independent effects of the surgical procedure on RFS, we used multivariate analyses with a Cox proportional hazards model. The SPSS software (version 10.5; SPSS, Inc., Chicago, IL, USA) was used for statistical analysis. Level of significance was set at a *P*-value of <0.05.

RESULTS

Of the 610 patients, 371 had radiologically determined solid-dominant tumours that had ≥50% solid component on HRCT analysis. Of these, 327 patients underwent lobectomy or segmentectomy and were analysed in this study (Fig. 1). No 30-day postoperative mortality was observed for the study subjects. The mean follow-up period after lobectomy and segmentectomy were 42.2 ± 16.4 months and 42.0 ± 19.2 months, respectively ($P = 0.79$).

The characteristics of the 327 patients are given in Table 1. Of these, 286 patients underwent lobectomy and 41 patients underwent segmentectomy. Lobectomy was performed significantly more often for patients with large whole and solid tumour size and high SUVmax tumours of clinical factors, and as a result, for those with vascular invasion and higher pathological stage. Details of procedures in segmentectomy are given in Table 2. One patient who underwent right S6 segmentectomy had lymph node involvement in Station 7. He developed multiple lung metastases 19.2 months after the operation. He has been receiving gefitinib and is alive and well without disease 43.3 months after the operation.

When comparing mixed GGO tumours with pure solid tumours, preoperative solid tumour size and SUVmax were significantly larger and carcinoembryonic antigen (CEA) was significantly higher in pure solid tumours. Regarding pathological factors, lymphatic invasion, vascular invasion, pleural invasion and lymph node metastasis were significantly more frequent in pure solid tumours (Table 3).

There was no significant difference in RFS between patients with a solid-dominant tumour who underwent lobectomy and those who underwent segmentectomy (3-year RFS, 84.4 vs 84.8%, respectively; $P = 0.69$, Fig. 2A). In patients with a mixed GGO tumour, there was no difference in RFS between patients who underwent lobectomy and those who underwent segmentectomy (3-year RFS, 91.0 vs 85.0%, respectively; $P = 0.60$, Fig. 2B). Even in patients with pure solid tumours, no significant difference in RFS was observed between the lobectomy and segmentectomy groups (3-year RFS, 76.8 vs 84.7%, respectively; $P = 0.48$, Fig. 2C). Univariate and multivariate analyses of RFS are given in Table 4. Multivariate analysis, including variables such as age, gender, solid tumour size on HRCT, SUVmax on FDG-PET/CT, tumour type, CEA and the surgical procedure, revealed that solid tumour size and SUVmax were independent prognostic factors for RFS ($P = 0.048$ and $P < 0.001$, respectively, Table 4).

Table 5 shows postoperative recurrence patterns between the patients who underwent lobectomy and those who underwent segmentectomy. No significant difference in local and distant recurrence rate was observed between the lobectomy and the segmentectomy groups (local, 5.6 vs 7.3%, $P = 0.72$; distant, 9.1 vs 4.9%, $P = 0.55$, respectively).

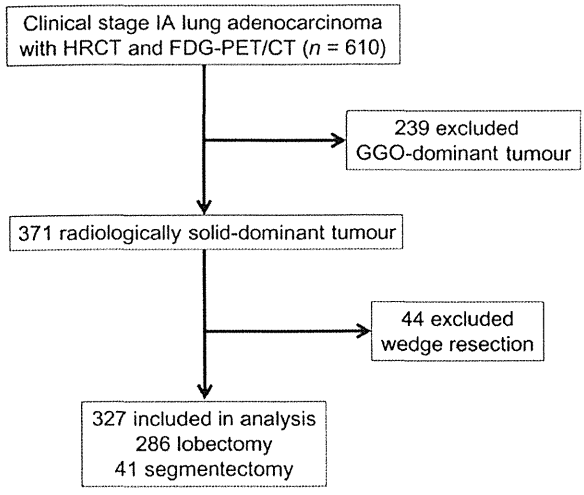

Figure 1: Flow chart of patients in the study.

DISCUSSION

In previous studies, GGO-dominant tumours were reported to be relatively benign tumours, which rarely have pathological invasiveness and lymph node metastasis, and are therefore suitable for sublobar resection such as wedge resection and segmentectomy [9]. On the other hand, radiologically determined solid-dominant tumours have a higher chance to exhibit pathological invasion such as lymphatic, vascular or pleural invasion and lymph node metastasis [8]. Indeed, about 20% of solid-dominant tumours had lymph node metastasis in this study. The prognostic significance of segmentectomy in such more malignant tumours is currently not well known. In the current study, the RFS of patients with solid-dominant tumour who underwent segmentectomy was similar to (no significant difference) that of those who underwent lobectomy.

Among radiologically determined solid-dominant tumours, pure solid tumours had a higher malignant potential than mixed tumours with GGO [15–17]. The present study also showed that pure solid tumours, which had a larger solid tumour size and

Table 1: Clinicopathological features of patients with solid-dominant tumours

	Solid-dominant tumours ($n = 327$)	Lobectomy ($n = 286$)	Segmentectomy ($n = 41$)	P-value[a]
Age	66 (33–86)	66 (33–84)	68 (45–86)	0.21
Gender, male	148 (45.2%)	126 (44.5%)	22 (53.7%)	0.31
Whole tumour size (cm)	2.1 (0.6–3.0)	2.2 (0.8–3.0)	1.6 (0.6–3.0)	<0.001
Solid tumour size (cm)	1.7 (0.5–3.0)	1.8 (0.6–3.0)	1.2 (0.5–3.0)	<0.001
SUVmax	2.3 (0–16.9)	2.5 (0–16.9)	1.6 (0–4.6)	<0.001
CEA (ng/ml)	2.6 (0–114)	2.6 (1.0–114)	2.4 (0–17)	0.28
Lymphatic invasion, positive	77 (23.5%)	71 (24.8%)	6 (14.6%)	0.17
Vascular invasion, positive	92 (28.1%)	86 (30.1%)	6 (16.8%)	0.042
Pleural invasion, positive	53 (16.2%)	49 (17.1%)	4 (9.8%)	0.36
Pathological stage				
IA	126 (38.5%)	98 (34.3%)	28 (68.3%)	<0.001
IB	162 (49.5%)	150 (52.4%)	12 (29.3%)	
IIA (N1)	18 (5.5%)	18 (6.3%)	0 (0%)	
IIIA (N2)	21 (6.4%)	20 (7.0%)	1 (2.4%)	

[a]Lobectomy vs segmentectomy.
GGO: ground-glass opacity; SUVmax: maximum standardized uptake value; CEA: carcinoembryonic antigen.

SUVmax, exhibited more pathological invasiveness and lymph node metastasis than mixed tumours. However, in pure solid tumours as well as mixed tumours, there was no significant difference in RFS between patients who underwent lobectomy and those who underwent segmentectomy. Interestingly, multivariate Cox proportional hazard model revealed that only solid tumour size on HRCT and SUVmax on FDG-PET/CT, and not tumour type (pure solid or mixed tumour) and the surgical procedure, were independent prognostic factors for RFS. In early lung adenocarcinoma, tumour types on HRCT are often classified as pure GGO, mixed GGO and pure solid tumour according to the GGO ratio, and these classifications represent their pathological malignancies well [16–18]. Actually, we reported that GGO-dominant lung adenocarcinoma rarely exhibited pathological invasiveness or lymph node metastasis regardless of solid tumour size and SUVmax [9]. However, in solid-dominant lung adenocarcinoma, solid tumour size on HRCT and SUVmax on FDG-PET/CT, rather than the presence of a GGO component, represent pathological malignancies. Solid tumour size on HRCT and SUVmax on FDG-PET/CT are important preoperative factors for early lung adenocarcinoma to predict pathological invasiveness, lymph node status and prognosis [11, 19–21]. In addition, the present study suggests that the RFS of segmentectomy is similar to that of lobectomy, even in more malignant populations such as those with large solid tumour sizes and high SUVmax.

When we apply segmentectomy to early lung cancers, we must avoid any recurrence in the residual pulmonary segments as much as possible. Although the recurrence patterns between lobectomy and segmentectomy groups were not significantly different, we experienced two recurrences in the residual segments after segmentectomy. Fortunately, those patients were treated with completion lobectomy and are alive and well without disease for 31 and 72 months after the initial operation. Because solid tumour size on HRCT and SUVmax on FDG-PET/CT were reported as independent prognostic factors for local RFS [6], patients with tumours with a large solid tumour size or a high SUVmax should carefully be chosen for segmentectomy. Taking wide surgical margins and intraoperative lymph node examinations using frozen sections are mandatory for such risky cases. When taking wide margins is difficult or lymph node metastasis is detected intraoperatively, the procedure should be converted to a lobectomy.

Because this was a retrospective study, patient selection for segmentectomy may have been very strict. Far degree of selection bias might lead to the results of this study, shown in baseline characteristics of patients (Table 1) between the lobectomy and segmentectomy groups. Also, to definitely conclude that segmentectomy does not worsen the prognosis when compared with lobectomy is difficult since the follow-up period is relatively short. We are eagerly awaiting the results of the large phase III trials, CALGB140503 in the USA and JCOG0802/WJOG4607L in Japan [22].

In conclusion, segmentectomy for solid-dominant clinical stage IA lung adenocarcinoma showed RFS equivalent to that of standard lobectomy in our selected patients. Segmentectomy can be performed even for a pure solid tumour under strict intraoperative lymph node examination. The prognosis of patients with a solid-dominant tumour depends on the solid tumour size on HRCT and SUVmax on FDG-PET/CT, rather than the surgical procedure.

Table 2: Details of procedures in segmentectomy

Site	*n*
Right	
S1	1
S2	8
S3	1
S6	9
S8 + 9	1
Left	
S1 + 2	4
S3	1
S1 + 2 + 3c	1
S1 + 2 + 3	4
S4	2
S5	1
S4 + 5	3
S6	2
S8	1
S9	2

Table 3: Comparison of clinicopathological factors between patients with mixed GGO tumours and those with pure solid tumours

	Mixed GGO tumours (*n* = 182)	Pure solid tumours (*n* = 145)	*P*-value
Age	66 (37–86)	66 (33–84)	0.70
Gender, male	74 (40.7%)	74 (51.0%)	0.06
Whole tumour size (cm)	2.1 (0.6–3.0)	2.0 (0.8–3.0)	0.50
Solid tumour size (cm)	1.5 (0.5–2.9)	2.0 (0.8–3.0)	<0.001
SUVmax	1.9 (0–12.4)	3.5 (0.4–16.9)	<0.001
CEA (ng/ml)	2.3 (1.0–25)	2.9 (0–114)	0.024
Procedure			
Lobectomy	154 (84.6%)	132 (91.0%)	0.08
Segmentectomy	28 (15.4%)	13 (9.0%)	
Lymphatic invasion, positive	26 (14.3%)	51 (35.2%)	<0.001
Vascular invasion, positive	34 (18.7%)	58 (40.0%)	<0.001
Pleural invasion, positive	18 (9.9%)	35 (24.1%)	<0.001
Lymph node metastasis, positive	11 (6.0%)	28 (19.3%)	<0.001

GGO: ground-glass opacity; SUVmax: maximum standardized uptake value; CEA: carcinoembryonic antigen.

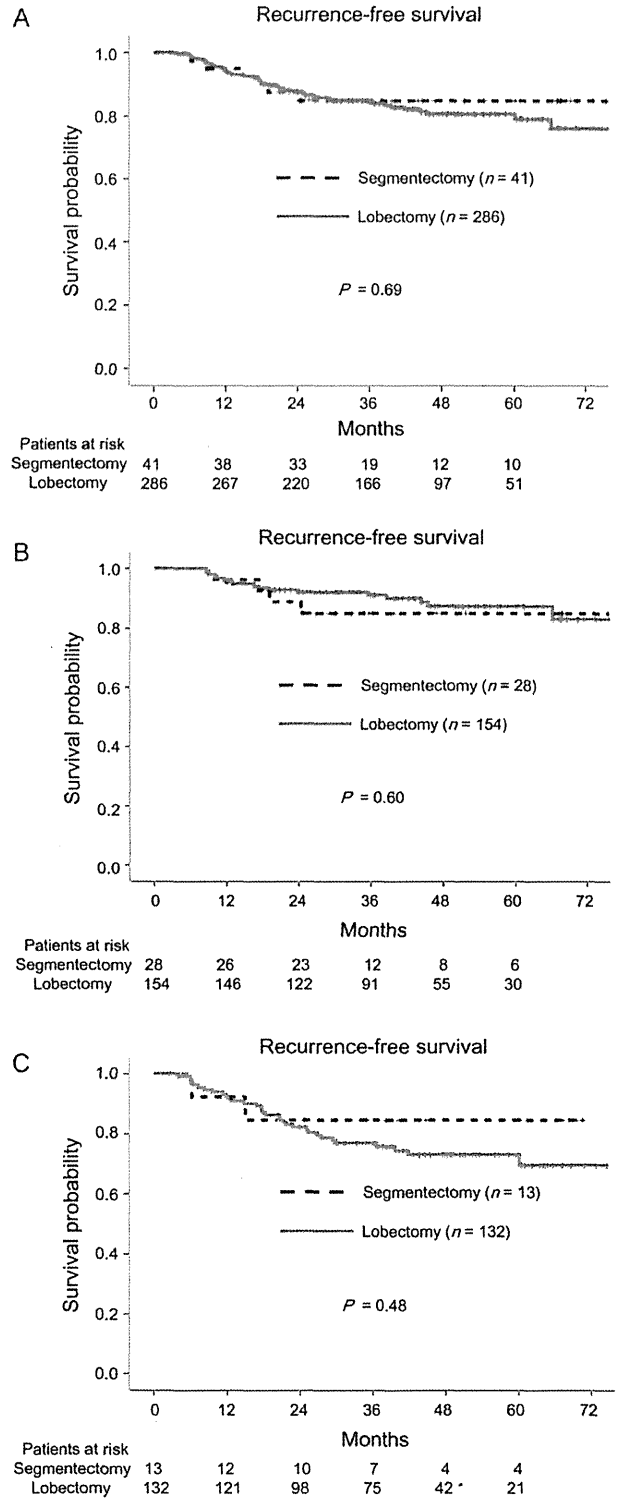

Figure 2: RFS curves for patients with solid-dominant tumours who underwent lobectomy and those who underwent segmentectomy. (**A**). In all cohorts, 3-year RFS rates of 84.4% (mean RFS of 64.7 months; 95% confidence interval [CI], 61.9–67.5 months) and 84.8% (mean RFS of 66.4 months; 95% CI, 59.5–73.1 months) were identified for patients who underwent lobectomy and those who underwent segmentectomy, respectively ($P = 0.69$). (**B**) In patients with mixed GGO tumours, 3-year RFS rates of 91.0% (mean RFS of 68.7 months; 95% CI, 65.6–71.8 months) and 85.0% (mean RFS of 66.8 months; 95% CI, 59.0–74.7 months) were identified for patients who underwent lobectomy and those who underwent segmentectomy, respectively ($P = 0.60$). (**C**) In patients with pure solid tumours, 3-year RFS rates of 76.8% (mean RFS of 59.4 months; 95% CI, 54.9–63.9 months) and 84.7% (mean RFS of 61.4 months; 95% CI, 49.6–73.2 months) were identified for patients who underwent lobectomy and those who underwent segmentectomy, respectively ($P = 0.48$).

Table 4: Univariate and multivariate analysis of RFS

Variables	HR (95% CI)	*P*-value
Univariate analysis		
Age	1.02 (0.99–1.05)	0.11
Gender, female (vs male)	1.11 (0.65–1.88)	0.70
Solid tumour size (cm)	2.07 (1..34–3.20)	0.001
SUVmax	1.17 (1.09–1.26)	<0.001
Tumour type, pure solid (vs Mixed GGO)	2.24 (1.30–3.85)	0.004
CEA (ng/ml)	1.01 (0.99–1.03)	0.36
Procedure, lobectomy (vs segmentectomy)	1.19 (0.51–2.78)	0.69
Multivariate analysis		
Age	1.02 (0.99–1.06)	0.18
Gender, female (vs male)	1.49 (0.82–2.71)	0.19
Solid tumour size (cm)	1.67 (1.01–2.88)	0.048
SUVmax	1.18 (1.08–1.29)	<0.001
Tumour type pure solid (vs mixed GGO)	1.31 (0.68–2.52)	0.42
CEA (ng/ml)	1.00 (0.96–1.04)	0.96
Procedure lobectomy (vs segmentectomy)	0.67 (0.27–1.70)	0.40

HR: hazard ratio; CI: confidence interval; SUVmax: maximum standardized uptake value; GGO: ground-glass opacity; CEA: carcinoembryonic antigen.

Table 5: Recurrence patterns between patients who underwent lobectomy and those who underwent segmentectomy

	Lobectomy (n = 286)	Segmentectomy (n = 41)	*P*-value
Local recurrence	16 (5.6%)	3 (7.3%)	0.72
Surgical stump	1	1	
Residual lung	0	1	
Pleura	3	1	
Lymph node	12	0	
Distant recurrence	26 (9.1%)	2 (4.9%)	0.55
Lung	10	1	
Bone	6	0	
Brain	3	0	
Meninges	0	1	
Adrenal grand	2	0	
Abdominal wall	1	0	
Lymph node	4	0	

Conflict of interest: none declared.

REFERENCES

[1] Jensik RJ, Faber LP, Milloy FJ, Monson DO. Segmental resection for lung carcinoma. A fifteen-year experience. J Thorac Cardiovasc Surg 1973;66: 563–72.

[2] Ginsberg RH, Rubinstein LV. Randomized trial of lobectomy versus limited resection for T1N0 non-small cell lung cancer. Lung Cancer Study Group. Ann Thorac Surg 1995;60:615–23.

[3] Okada M, Koike T, Higashiyama M, Yamato Y, Kodama K, Tsubota N. Radical sublobar resection for small-sized non-small cell lung cancer: a multicenter study. J Thorac Cardiovasc Surg 2006;132:769–75.

[4] Okada M, Tsutani Y, Ikeda T, Misumi K, Matsumoto K, Yoshimura M *et al.* Radical hybrid video-assisted thoracic segmentectomy: long-term results of minimally invasive anatomical sublobar resection for treating lung cancer. Interact CardioVasc Thorac Surg 2012;14:5–11.

[5] Whitson BA, Groth SS, Andrade RS, Maddaus MA, Habermann EB, D'Cunha J. Survival after lobectomy versus segmentectomy for stage I non-small cell lung cancer: a population-based analysis. Ann Thorac Surg 2011;92:1943–50.

[6] Tsutani Y, Miyata Y, Nakayama H, Okumura S, Adachi S, Yoshimura M *et al.* Oncologic outcomes of segmentectomy compared with lobectomy for clinical stage IA lung adenocarcinoma: propensity score-matched analysis in a multicenter study. J Thorac Cardiovasc Surg 2013;146:358–64.

[7] Kodama K, Higashiyama M, Yokouchi H, Takami K, Kuriyama K, Mano M *et al.* Prognostic value of ground-glass opacity found in small lung adenocarcinoma on high-resolution CT scanning. Lung Cancer 2001;33:17–25.

[8] Asamura H, Hishida T, Suzuki K, Koike T, Nakamura K, Kusumoto M *et al.* Radiographically determined noninvasive adenocarcinoma of the lung: survival outcomes of Japan Clinical Oncology Group 0201. J Thorac Cardiovasc Surg 2013;146:24–30.

[9] Tsutani Y, Miyata Y, Nakayama H, Okumura S, Adachi S, Yoshimura M *et al.* Appropriate sublobar resection choice for ground glass opacity-dominant clinical stage IA lung adenocarcinoma: wedge resection or segmentectomy. Chest 2013;doi: 10.1378/chest. 13-1094.

[10] Goldstraw P, Crowley J, Chansky K, Giroux DJ, Groome PA, Rami-Porta R *et al.* International Association for the Study of Lung Cancer International Staging Committee; Participating Institutions. The IASLC Lung Cancer Staging Project: proposals for the revision of the TNM stage groupings in the forthcoming (seventh) edition of the TNM Classification of Malignant Tumours. J Thorac Oncol 2007;2:706–14.

[11] Tsutani Y, Miyata Y, Nakayama H, Okumura S, Adachi S, Yoshiura M *et al.* Prognostic significance of using solid versus whole tumor size on high-resolution computed tomography for predicting the pathological malignant grade of tumors in clinical stage IA lung adenocarcinoma: a multicenter study. J Thorac Cardiovasc Surg 2012;143:607–12.

[12] Delbeke D, Coleman RE, Guiberteau MJ, Brown ML, Royal HD, Siegel BA *et al.* Procedure guideline for tumor imaging with 18F-FDG PET/CT 1.0. J Nucl Med 2006;47:885–95.

[13] Mawlawi O, Podoloff DA, Kohlmyer S, Williams JJ, Stearns CW, Culp RF *et al.* Performance characteristics of a newly developed PET/CT scanner using NEMA standards in 2D and 3D modes. J Nucl Med 2004;45:1734–42.

[14] Okada M, Nakayama H, Okumura S, Daisaki H, Adachi S, Yoshimura M *et al.* Multicenter analysis of high-resolution computed tomography and positron emission tomography/computed tomography findings to choose therapeutic strategies for clinical stage IA lung adenocarcinoma. J Thorac Cardiovasc Surg 2011;141:1384–91.

[15] Inoue M, Minami M, Sawabata N, Utsumi T, Kadota Y, Shigemura N *et al.* Clinical outcome of resected solid-type small-sized c-stage IA non-small cell lung cancer. Eur J Cardiovasc Surg 2010;89:1312–9.

[16] Hattori A, Suzuki K, Matsunaga T, Fukui M, Kitamura Y, Miyasaka Y *et al.* Is limited resection appropriate for radiologically 'solid' tumors in small lung cancers? Ann Thorac Surg 2012;94:212–5.

[17] Tsutani Y, Miyata Y, Yamanaka T, Nakayama H, Okumura S, Adachi S *et al.* Solid tumors versus mixed tumors with a ground-glass opacity component in patients with clinical stage IA lung adenocarcinoma: prognostic comparison using high-resolution computed tomography findings. J Thorac Cardiovasc Surg 2013;146:17–23.

[18] Suzuki K, Kusumoto M, Watanabe S, Tsuchiya R, Asamura H. Radiologic classification of small adenocarcinoma of the lung: radiologic-pathologic correlation and its prognostic impact. Ann Thorac Surg 2006;81:413–9.

[19] Tsutani Y, Miyata Y, Misumi K, Ikeda T, Mimura T, Hihara J *et al.* Difference in prognostic significance of maximum standardized uptake value on [18F]-fluoro-2-deoxyglucose positron emission tomography between adenocarcinoma and squamous cell carcinoma of the lung. Jpn J Clin Oncol 2011;41:890–6.

[20] Tsutani Y, Miyata Y, Nakayama H, Okumura S, Adachi S, Yoshimura M *et al.* Prediction of pathological node-negative clinical stage IA lung adenocarcinoma for optimal candidates undergoing sublobar resection. J Thorac Cardiovasc Surg 2012;144:1365–71.

[21] Tsutani Y, Miyata Y, Nakayama H, Okumura S, Adachi S, Yoshimura M *et al.* Solid tumor size on high-resolution computed tomography and maximum standardized uptake value on positron emission tomography for new clinical T descriptors with T1 lung adenocarcinoma. Ann Oncol 2013;24:2376–81.

[22] Nakamura K, Saji H, Nakajima R, Okada M, Asamura H, Shibata T *et al.* A phase III randomized trial of lobectomy versus limited resection for small-sized peripheral non-small cell lung cancer (JCOG0802/WJOG4607L). Jpn J Clin Oncol 2010;40:271–4.

Asian Cardiovascular and Thoracic Annals
http://aan.sagepub.com/

Prophylaxis for acute exacerbation of interstitial pneumonia after lung resection

Hiroyuki Ito, Haruhiko Nakayama, Tomoyuki Yokose and Kouzo Yamada

Asian Cardiovascular and Thoracic Annals published online 20 February 2014
DOI: 10.1177/0218492314526187

The online version of this article can be found at:
http://aan.sagepub.com/content/early/2014/02/20/0218492314526187

Published by:
SAGE
http://www.sagepublications.com

On behalf of:

The Asian Society for Cardiovascular Surgery

Original Article

ASIAN CARDIOVASCULAR & THORACIC ANNALS

Asian Cardiovascular & Thoracic Annals
0(0) 1–7

DOI: 10.1177/0218492314526187
aan.sagepub.com
SAGE

Prophylaxis for acute exacerbation of interstitial pneumonia after lung resection

Hiroyuki Ito[1], Haruhiko Nakayama[1], Tomoyuki Yokose[2] and Kouzo Yamada[3]

Abstract

Background and purpose: Acute exacerbation of interstitial pneumonia is a life-threatening complication after lung cancer surgery. Dorsal subpleural fibrotic changes occupying 3 or more segments of both lower lobes on high-resolution computed tomography indicate a very high risk. We conducted a prospective phase II study to assess the efficacy of prophylactic treatment.

Methods: Patients with lung cancer underwent high-resolution computed tomography preoperatively to assess the risk of acute exacerbations of interstitial pneumonia. Before induction of general anesthesia, high-risk patients received 125 mg of methylprednisolone as an intravenous bolus and sivelestat sodium hydrate 300 $mg \cdot day^{-1}$ as a continuous intravenous infusion. From January 2010 through August 2011, a total of 327 patients underwent surgery for lung cancer, and 31 (9.5%) were enrolled.

Results: There was no case of acute exacerbation. No adverse events were associated with prophylaxis. Usual interstitial pneumonia was confirmed histopathologically in 25 (80.6%) patients. Four (12.9%) patients had major complications. Usual interstitial pneumonia was diagnosed postoperatively in 4 (1.4%) of 327 patients who did not meet the inclusion criteria, and 1 of these patients died due to acute exacerbation of occult interstitial pneumonia.

Conclusion: Perioperative use of sivelestat sodium hydrate and low-dose methylprednisolone may be useful as prophylaxis for acute exacerbation of interstitial pneumonia.

Keywords

Interstitiall lung diseases, lung neoplasms, pulmonary fibrosis, postoperative complications

Surgery remains the standard treatment for early stage primary lung cancer. Recent improvements in patient selection criteria, operative techniques, and postoperative management have contributed to lower mortality. In 1999, an analysis of data from a Japanese lung cancer registry estimated that mortality had decreased to 0.9%.[1] Respiratory complications are very common, and approximately half of all postoperative deaths are attributed to interstitial pneumonia (IP).[2] Apparent IP, as represented by idiopathic pulmonary fibrosis (IPF), is an important risk factor for postoperative mortality; postoperative acute exacerbation of interstitial pneumonia (AE-IP) is a life-threatening complication after lung cancer surgery.[3,4] We previously reported that dorsal subpleural fibrotic changes occupying 3 or more segments in both lower lobes (honeycombing) on high-resolution computed tomography (HRCT) and operative time are clinically significant risks factor for AE-IP in patients with lung cancer;[5] the incidence of postoperative AE-IP among patients with CT honeycombing was 10.9% (5/46), 80% of whom died of AE-IP. The onset of AE-IP in patients with occult IPF leads to poor outcomes despite medical therapy. At present, effective treatments for AE-IP remain to be established.[6–10] We conducted a prospective phase II study to assess the efficacy of prophylactic treatment

[1]Department of Thoracic Surgery, Kanagawa Cancer Center, Yokohama, Japan
[2]Department of Pathology, Kanagawa Cancer Center, Yokohama, Japan
[3]Department of Thoracic Oncology, Kanagawa Cancer Center, Yokohama, Japan

Corresponding author:
Hiroyuki Ito, MD, Department of Thoracic Surgery, Kanagawa Cancer Center, 2-3-2 Nakao, Asahi-ku, Yokohama, Japan 241-8515.
Email: h-ito@kcch.jp

against postoperative AE-IP in patients with CT honeycombing who were treated in a single center.

Patients and methods

Our institutional internal review board approved this prospective study (institutional acceptance number Ken-24, 2009), and written informed consent was obtained from all patients. From January 2010 through August 2011, 327 patients underwent surgical treatment for lung cancer at our hospital. Tumors were staged according to the 7th UICC TNM staging system.

All patients had resectable non-small-cell lung cancer. Patients at high risk of postoperative AE-IP were identified on the basis of HRCT findings. Both lungs were examined within 1 month before surgery. The conditions of HRCT were a slice thickness of 3 mm or thinner, and use of the same window settings. HRCT scans were double-checked by a pulmonologist and a surgeon. The criteria for CT honeycombing in this study were dorsal and focal or diffuse subpleural honeycomb formation with or without fibrotic changes, occupying 3 or more segments of both lower lobes (Figure 1). Curvilinear shadows and dependent densities indicating gravitational effects were excluded. We excluded patients with currently treated IP, a treatment history of IP within the past 5 years, and a history of induction therapy, chemotherapy, or radiotherapy for any type of thoracic malignancy. Patients with unstable ischemic heart disease, a history of acute myocardial infarction within the past 3 months, heart failure, unstable arrhythmias, poorly controlled diabetes mellitus, or uncontrolled infectious disease, and pregnant women were also excluded. All patients underwent a preoperative functional cardiologic evaluation and pulmonary function testing. Lobectomy with systematic mediastinal lymph node dissection was the standard procedure. In patients with complications, wide wedge resection or segmentectomy was performed to achieve complete resection with definite surgical margins.

Most cases of AE-IP develop within several weeks after the operation,[5–7] a time associated with high levels of cytokines. During surgery and in the early postoperative period, a number of cytokines are released. These mediators of the host defense response of mesenchymal cells induce deposition of extracellular matrix products and collagen, resulting in fibrosis. This might the one of the causes of postoperative acute exacerbation of interstitial lung disease. The postoperative host defense response is most likely a major contributing factor to AE-IP. We hypothesized that suppressing the postoperative inflammatory response during operation and in the early postoperative period was the key to reducing the risk of postoperative AE-IP. Sivelestat sodium hydrate (sodium N-{2-[4-(2, 2-dimethylpropionyloxy) phenylsulfonylamino] benzoyl} aminoacetate tetra hydrate (Elaspol, ONO-5046-Na [C20H21N2NaO7S-Na-4H2O, molecular weight, 528.51]; Ono Pharmaceutical Co., Osaka, Japan) was developed as a specific inhibitor of neutrophil elastase, an extremely cytotoxic enzyme in plasma and interstitial fluid.[11] Sivelestat competitively inhibits the activity of neutrophil elastase in humans, but it does not affect other proteases.[12,13] Sivelestat has been approved in Japan for the indications of acute lung injury (ALI) and acute respiratory distress syndrome ARDS).[14] Although there have been conflicting results regarding its benefits,[15] a Japanese phase III trial demonstrated that sivelestat was effective in patients with ALI/ARDS

Figure 1. Preoperative high-resolution computed tomography in 3 patients with computed tomography honeycombing. Diffuse subpleural dorsal honeycombing with focal fibrotic changes can be seen.

associated with systemic inflammatory response syndrome. The benefits of sivelestat include improved pulmonary oxygenation, a reduced duration of mechanical ventilation, and a shorter stay in the intensive care unit (ICU).[14] These results suggest that sivelestat could potentially suppress the severe inflammatory response after highly invasive operations such as thoracotomy. In addition, serum levels of inflammatory cytokines such as interleukin-1b and neutrophil elastase are suppressed by treatment with sivelestat.[13] Serious adverse events associated with sivelestat include dyspnea (0.2%), leukopenia (0.2%), thrombocytopenia (0.2%), and severely impaired liver function (0.2%). Corticosteroids inhibit the host defense response at many levels, and suppress fibrogenesis and the expression of adhesion molecules.[16] Treatment with corticosteroids did not reduce mortality in patients with ARDS,[17,18] but low-dose corticosteroids in the early stage of ARDS was found to lead to complete maintenance of respiratory mechanics in mild ALI, as well as minimal changes in tissue impedance and extracellular matrix components in severe lesions.[19] The use of low-dose methylprednisolone in early postoperative ARDS has produced favorite outcomes by significantly reducing postoperative mortality and promoting recovery without mechanical ventilation.[9]

We studied whether the perioperative combined use of sivelestat and low-dose methylprednisolone reduced postoperative levels of inflammatory cytokines in patients with lung cancer who were preoperatively identified to be at high risk of acute exacerbations of interstitial lung disease. Immediately before induction of general anesthesia, 125 mg of methylprednisolone was given as an intravenous bolus and 300 $mg \cdot day^{-1}$ of sivelestat was administered as a continuous intravenous infusion. Sivelestat was continued for 48 h; this period is associated with high levels of postoperative cytokines.

Preoperative assessments, surgery, anesthesia, and postoperative management were performed by the same anesthesia and surgical team in all patients. Postoperatively, patients were admitted to the ICU for that day only. Transfusion was performed at a rate of 1.25 $mL \cdot kg^{-1} \cdot h^{-1}$, and the patient wore an oxygen (40%) mask until the next morning. As routinely performed for postoperative patients, percutaneous oxygen saturation (SpO_2) and chest radiography were performed on postoperative days 0, 1, 4, and 7. Laboratory values were checked on postoperative days 1, 4, and 7. Discharge was scheduled for postoperative day 7. Chest CT was performed immediately if the SpO_2 was <93% while breathing room air or an infiltrating shadow was noted on chest radiography. Sputum cultures were examined or bronchofibroscopy was performed to exclude the possibility of aspiration and bacterial infection. Cardiac ultrasonography was performed to rule out acute heart failure. Patients were closely monitored postoperatively, and adverse events were graded according to the Common Terminology Criteria for Adverse Events version 4.0. Any grade 2 or higher complications were recorded as postoperative complications. In addition to routine histological examinations and staging, lung specimens from all patients were histopathologically examined for evidence suggesting IP, especially usual interstitial pneumonia (UIP), a typical histological finding of IPF. If honeycomb lesions seen on CT were not included in the specimens resected at lung cancer surgery, an additional partial resection, such as biopsy of a lower lobe, was performed to confirm the presence of IP.

The primary endpoint was the incidence of AE-IP within 30 days after surgery. Secondary endpoints were the diagnostic accuracy of UIP on HRCT, postoperative morbidity, and mortality. The expected incidence of AE-IP within 30 days after operation was assumed to be less than 1%, with a threshold value of 10% or higher. A sample size of 30 patients was calculated to be necessary, with an alpha error of 0.05 and a beta error of 0.2. Postoperative AE-IP was diagnosed on the basis of acute hypoxia-like ALI/ARDS; a PaO_2-to-fraction of inspired O_2 ratio <300 with bilateral infiltrations on chest radiography; and the involvement of both lungs. AE-IP caused by aspiration, bacterial infection, or acute heart failure was excluded. We also studied patients' clinical characteristics (age, sex, smoking history, PaO_2, % of predicted forced vital capacity, % of predicted forced expiratory volume in 1 s, coexisting heart disease, TNM stage), preoperative laboratory data, and surgical records (operation time, blood loss, extent of surgery, blood transfusion). Postoperative morbidity and mortality were defined as events occurring within 30 days after operation. Each variable was tested by the chi-square test, Fisher's exact test, or Student's t test. Logistic-regression analysis was used for multivariate analysis and performed with StatView for Windows version 5.0 (SAS Institute, Inc., Cary, NC, USA). Statistical significance was defined as a p value of less than 0.05.

Results

During the study period, 31 (9.5%) patients were enrolled. Table 1 shows the clinical characteristics of these patients. All were smokers, and many had several cardiopulmonary comorbidities; only 4 were free of comorbidities. On spirography, 23 (74.2%) patients showed normal function, but the mean diffusing capacity for carbon monoxide was decreased to 75.3% ±22.5%, which tended to be lower than that in other

Table 1. Characteristics of 31 patients at high risk of acute exacerbation of interstitial pneumonia.

Variable	No. of patients	Mean [range]
Sex (male/female)	30/1	
Age (years)		72.3 ± 6.49 [61–86]
Smoker	31 (100%)	
Smoking index		1087 ± 597 [210–2700]
%FVC		99.0% ±17.2% [62.4%–129%]
$\%FEV_1$		76.4% ±6.2% [64.0%–94.9%]
%DLCO		75.3% ±22.5% [34.8%–140%]
Spirogram pattern		
Normal	23	
Obstructive	2	
Restrictive	5	
Combined	1	
Clinical stage		
IA	10	
IB	7	
IIA	8	
IIB	3	
IIIA	3	
Elevated WBC	0	
Elevated CRP ($mg \cdot dL^{-1}$)	13	1.27 [0.33–4.87]
Elevated LDH ($U \cdot L^{-1}$)	3	275.3 [260–290]
Elevated KL-6 ($U \cdot mL^{-1}$)	17	788 [504–1360]
Comorbidities*		
Emphysema	18	
Hypertension	9	
Diabetes	5	
Ischemic heart disease	4	
Bronchial asthma	3	
Tuberculosis	3	
Arrhythmia	3	
Ischemic cerebral disease	2	
Hepatitis	2	
Rheumatoid arthritis	1	
Abdominal aortic aneurysm	1	
Extent of surgery		
Lobectomy	22	
Segmentectomy	3	
Wide wedge resection	6	

*There was some overlap. CRP: C-reactive protein; %DLCO: % of predicted diffusing capacity of the lung for carbon monoxide; %FVC: % of predicted forced vital capacity; $\%FEV_1$: % of predicted forced expiratory volume in 1 s; LDH: lactate dehydrogenase; KL-6: sialylated carbohydrate antigen KL-6; WBC: white blood cells.

patients with lung cancer. Wide wedge resection was performed in 6 patients, and segmentectomy was performed in 3 because of lower cardiopulmonary reserve and comorbidities. The mean operation time was 144 ± 62.0 min (range 36–280 min), the mean blood loss was 35.0 ± 34.0 g (range 5–130 g), and no patient received a blood transfusion. There was no case of postoperative AE-IP. Major morbidity occurred in 4 (12.9%) patients. One (3.2%) patient had a myocardial infarction (grade 5) on postoperative day 29 and died within 30 days after operation. Another patient had a bronchopleural fistula (grade 5) after a right lower

lobectomy; bacterial pneumonia developed, and the patient died 43 days after the operation. Other major morbidities were cerebral infarction (cerebrovascular ischemia grade 2) in one patient, and prolonged air leakage requiring pleurodesis (pulmonary fistula grade 2) in another. The Data and Safety Monitoring Committee concluded that these complications were not clearly but possibly related to prophylaxis. These two patients were originally thought to be at high risk for lung cancer surgery. They had several comorbidities: one had ischemic heart disease with past history of acute myocardial infarction, emphysema, and diabetes mellitus; and the other had history of heavy smoking and hypertension, and the operative procedure was a right lower lobectomy which carries a risk of bronchopleural fistula. None of the variables we tested showed statistical significance regarding the incidence of postoperative death. Besides these morbidities, there was no other grade 2 or higher adverse effect. UIP was histopathologically confirmed in 25 (80.6%) patients. Three patients were confirmed to have nonspecific interstitial pneumonia, and 3 had smoking-related interstitial fibrosis of the lung. The overall diagnostic accuracy of IP on HRCT was 90.3% (28/31). The mean postoperative hospital stay was 8.2 ± 5.2 days (range 4–30 days), and the ICU stay was 1.1 days (range 1–2 days). Four of 327 (1.4%) patients who did not meet the HRCT criteria were postoperatively given a diagnosis of UIP on histopathological examination; one of these had postoperative acute exacerbation of UIP and died of respiratory failure on postoperative day 42. During this period, 2 patients with currently treated apparent IPF were excluded from this study. A lobectomy and a partial resection were performed; AE-IP did not develop in either of these patients. The overall operative mortality was 0.9%.

Discussion

The incidence of postoperative mortality related to AE-IP remains high; this is a major problem that needs to be overcome in thoracic surgery. Once postoperative AE-IP develops, even in the presence of occult or apparent IPF, mortality is extremely high.[5–7] Perioperative use of sivelestat and low-dose methylprednisolone may be useful as prophylaxis against AE-IP in high-risk patients. Retrospective studies have reported that the postoperative administration of sivelestat increases oxygenation, reduces the duration of mechanical ventilation, and shortens the ICU stay in patients who undergo thoracic surgery.[13,20] However, in our previous study, patients with UIP who had ALI/ARDS postoperatively received sivelestat and steroids, but mortality was high,[5] consistent with the results of the STRIVE study.[15] This finding implies that starting treatment with sivelestat after the onset of AE-IP is too late. To our knowledge, the value of prophylactic therapy in patients with occult IPF who undergo lung cancer surgery has not been evaluated previously. In this sense, the results of our trial are very promising.

The mechanism of AE-IP remains unclear, but several factors appear to be involved. Representative factors include highly invasive procedures and treatment such as pneumonectomy, induction therapy, prolonged operations, and high blood loss.[6,21] Besides countermeasures against postoperative AE-IP in patients with occult IPF, careful postoperative management should be implemented. Avoiding excessive perioperative fluid administration also has an important role in reducing the risk of AE-IP.[22] In this study, a single integrated surgical team performed postoperative fluid management by controlling the infusion rate and checking the body weight of all patients.

The detailed images obtained on HRCT were very useful for detecting IPF. In a previous study, we showed that focal dorsal subpleural honeycombing occupying 3 or more segments of both lower lobes on HRCT suggests the presence of occult IPF. CT honeycombing on HRCT is a simple and useful predictor of the risk of postoperative AE-IP. Measures to prevent postoperative AE-IP in patients with occult IPF are essential to improve the safety of lung cancer surgery. In the present study, the presence or absence of UIP was confirmed histopathologically in all patients with evidence of UIP on HRCT, and UIP was accurately detected in 80% of patients. Three patients were given a diagnosis of smoking-related interstitial fibrosis, which is a distinct form of chronic interstitial fibrosis that is common in smokers.[23,24] This is not a critical disease nor related to AE-IP, but smoking-related interstitial fibrosis may rarely present with radiologic findings similar to those associated with UIP; it is therefore difficult to distinguish smoking-related interstitial fibrosis from occult IPF in some patients. Nearly all of our patients were men and heavy smokers who had several comorbidities, including vascular disease, cardiopulmonary disease, and diabetes. The Data and Safety Monitoring Committee concluded that these were possibly related to prophylaxis because of the high incidence of postoperative death; we thought the subjects of our study were a group of very high-risk patients for lung cancer surgery. The high mortality and major morbidity rates in this study can thus probably be attributed to the need for prophylaxis against AE-IP combined with other high-risk factors. When such patients are scheduled to undergo lung cancer surgery, it is essential to obtain fully informed consent and to

perform thorough preoperative evaluation and careful postoperative management.

Our study had several important limitations. Although this trial was prospective and achieved our main objectives, the sample size was small, the study was performed at a single center, and the accuracy of our data is considered inadequate. We performed this trial as a pilot study, given the small number of target patients. Our findings should be confirmed in larger prospective multicenter clinical trials involving sufficient numbers of patients. Nevertheless, we concluded that perioperative administration of sivelestat sodium hydrate and low-dose methylprednisolone may be useful as prophylaxis against AE-IP in high-risk patients who undergo lung cancer surgery. The patients who could be enrolled for this prophylaxis were thought to be at very high risk of postoperative mortality, thus physicians should pay much attention to preoperative evaluation and postoperative management.

Funding

This research received no specific grant from any funding agency in the public, commercial, or not-for-profit sectors.

Conflicts of interest statement

None declared.

References

1. Koike T, Yamato Y, Asamura H, et al. Improvements in surgical results for lung cancer from 1989 to 1999 in Japan. *J Thorac Oncol* 2009; 4: 1364–1369.
2. Watanabe S, Asamura H, Suzuki K and Tsuchiya R. Recent results of postoperative mortality for surgical resections in lung cancer. *Ann Thorac Surg* 2004; 78: 999–1002.
3. Kudoh S, Kato H, Nishiwaki Y, et al. Interstitial lung disease in Japanese patients with lung cancer: a cohort and nested case-control study. *Am J Respir Crit Care Med* 2008; 177: 1348–1357.
4. Watanabe A, Higami T, Ohori S, et al. Is lung cancer resection indicated in patients with idiopathic pulmonary fibrosis? *J Thorac Cardiovasc Surg* 2008; 136: 1357–1363.
5. Ito H, Nakayama H, Tsuboi M, et al. Subpleural honeycombing on high resolution computed tomography is risk factor for fatal pneumonitis. *Ann Thorac Surg* 2011; 91: 874–878.
6. Chida M, Ono S, Hoshikawa Y and Kondo T. Subclinical idiopathic pulmonary fibrosis is also a risk factor of postoperative acute respiratory distress syndrome following thoracic surgery. *Eur J Cardiothorac Surg* 2008; 34: 878–881.
7. Tanita T, Chida M, Hoshikawa Y, et al. Experience with fatal interstitial pneumonia after operation for lung cancer. *J Cardiovasc Surg* 2001; 42: 125–129.
8. Deslauriers J and Mehran R. *Handbook of perioperative care in general thoracic surgery*. Philadelphia: Elsevier Mosby, 2005, pp. 314–317.
9. Lee HS, Lee JM, Kim MS, Kim HY, Hwangbo B and Zo JI. Low-dose steroid therapy at an early phase of postoperative acute respiratory distress syndrome. *Ann Thorac Surg* 2005; 79: 405–410.
10. Kutlu CA, Williams EA, Evans TW, Pastorino U and Goldstraw P. Acute lung injury and acute respiratory distress syndrome after pulmonary resection. *Ann Thorac Surg* 2000; 69: 376–380.
11. Kawabata K, Suzuki M, Sugitani M, Imaki K, Toda M and Miyamoto T. ONO-5046, a novel inhibitor of human neutrophil elastase. *Biochem Biophys Res Commun* 1991; 177: 814–820.
12. Matsuzaki K, Hiramatsu Y, Homma S, Sato S, Shigeta O and Sakakibara Y. Sivelestat reduces inflammatory mediators and preserves neutrophil deformability during simulated extracorporeal circulation. *Ann Thorac Surg* 2005; 80: 611–617.
13. Suda K, Kitagawa Y, Ozawa S, et al. Neutrophil elastase inhibitor improves postoperative clinical courses after thoracic esophagectomy. *Dis Esophagus* 2007; 20: 478–486.
14. Tamakuma S, Ogawa M, Aikawa N, et al. Relationship between neutrophil elastase and acute lung injury in humans. *Pulm Pharmacol Ther* 2004; 17: 271–279.
15. Zeiher BG, Artigas A, Vincent JL, et al. Neutrophil elastase inhibition in acute lung injury: results of the STRIVE study. *Crit Care Med* 2004; 32: 1695–1702.
16. Jantz MA and Sahn SA. Corticosteroids in acute respiratory failure. *Am J Respir Crit Care Med* 1999; 160: 1079–1100.
17. Luce JM, Montgomery AB, Marks JD, Turner J, Metz CA and Murray JF. Ineffectiveness of high-dose methylprednisolone in preventing parenchymal lung injury and improving mortality in patients with septic shock. *Am Rev Respir Dis* 1988; 138: 62–68.
18. Bernard GR, Luce JM, Sprung CL, et al. High-dose corticosteroids in patients with the adult respiratory distress syndrome. *N Engl J Med* 1987; 317: 1565–1570.
19. Rocco PR, Souza AB, Faffe DS, et al. Effect of corticosteroid on lung parenchyma remodeling at an early phase of acute lung injury. *Am J Respir Crit Care Med* 2003; 168: 677–684.
20. Ono S, Tsujimoto H, Hiraki S, et al. Effects of neutrophil elastase inhibitor on progression of acute lung injury following esophagectomy. *World J Surg* 2007; 31: 1996–2001.
21. Muraoka M, Tagawa T, Akamine S, et al. Acute interstitial pneumonia following surgery for primary lung cancer. *Eur J Cardiothorac Surg* 2006; 30: 657–662.
22. Mizuno Y, Iwata H, Shirahashi K, et al. The importance of intraoperative fluid balance for the prevention of postoperative acute exacerbation of idiopathic pulmonary fibrosis after pulmonary resection for primary lung cancer. *Eur J Cardiothorac Surg* 2012; 41: e161–e165.

23. Katzenstein AL, Mukhopadhyay S, Zanardi C and Dexter E. Clinically occult interstitial fibrosis in smokers: classification and significance of a surprisingly common finding in lobectomy specimens. *Hum Pathol* 2010; 41: 316–325.

24. Katzenstein AL. Smoking-related interstitial fibrosis (SRIF), pathogenesis and treatment of usual interstitial pneumonia (UIP), and transbronchial biopsy in UIP [Review]. *Mod Pathol* 2012; 25(Suppl 1): S68–S78.

Reproducibility of Histopathological Diagnosis in Poorly Differentiated NSCLC

An International Multiobserver Study

Erik Thunnissen, MD, PhD, Masayuki Noguchi, MD,† Seena Aisner, MD,‡ Mary Beth Beasley, MD,§ Elisabeth Brambilla, MD, PhD,‖ Lucian R. Chirieac, MD,¶ Jin-Haeng Chung, MD, PhD,# Sanja Dacic, MD,** Kim R. Geisinger, MD,†† Fred R. Hirsch, MD, PhD,‡‡ Yuichi Ishikawa, MD, PhD,§§ Keith M. Kerr, MD, PhD,‖ Sylvie Lantejoul, MD, PhD,¶¶ Yoshiro Matsuno, MD,## Yuko Minami, MD,*** Andre L. Moreira, MD,††† Giuseppe Pelosi, MD,‡‡‡ Iver Petersen, MD, PhD,§§§ Victor Roggli, MD,‖‖‖ William D. Travis, MD,††† Ignacio Wistuba, MD,¶¶¶ Yasushi Yatabe, MD, PhD,### Rafal Dziadziuszko, MD, PhD,**** Birgit Witte, PhD,†††† Ming-Sound Tsao, MD, FRCPC,‡‡‡‡ and Andrew G. Nicholson, DM,§§§§*

Introduction: The 2004 World Health Organization classification of lung cancer contained three major forms of non–small-cell lung cancer: squamous cell carcinoma (SqCC), adenocarcinoma (AdC), and large cell carcinoma. The goal of this study was first, to assess the reproducibility of a set of histopathological features for SqCC in relation to other poorly differentiated non–small-cell lung cancers and second, to assess the value of immunohistochemistry in improving the diagnosis.

Methods: Resection specimens (n = 37) with SqCC, large cell carcinoma, basaloid carcinoma, sarcomatoid carcinoma, lymphoepithelial-like carcinoma, and solid AdC, were contributed by the participating pathologists. Hematoxylin and eosin (H&E) stained slides were digitized. The diagnoses were evaluated in two ways. First, the histological criteria were evaluated and the (differential) diagnosis on H&E alone was scored. Second, the added value of additional stains to make an integrated diagnosis was examined.

Results: The histologic criteria defining SqCC were consistently used, but in poorly differentiated cases they were infrequently present, rendering the diagnosis more difficult. Kappa scores on H&E alone were for SqCC 0.46, large cell carcinoma 0.25, basaloid carcinoma 0.27, sarcomatoid carcinoma 0.52, lymphoepithelial-like carcinoma 0.56, and solid AdC 0.21. The κ score improved with the use of additional stains for SqCC (combined with basaloid carcinoma) to 0.57, for solid AdC to 0.63.

Conclusion: The histologic criteria that may be used in the differential diagnosis of poorly differentiated lung cancer were more precisely refined. Furthermore, additional stains improved the reproducibility of histological diagnosis of SqCC and AdC, uncovering information that was not present in routine H&E stained slides.

Key Words: Non–small-cell lung cancer, Pathology, Reproducibility.

(*J Thorac Oncol.* 2014;9: 1354–1362)

Departments of *Pathology and ††††Epidemiology and Biostatistics, VU University Medical Centre, Amsterdam, The Netherlands; †Department of Pathology, Faculty of Medicine, Tsukuba, Japan; ‡Rutgers New Jersey Medical School, Newark, New Jersey; §Department of Pathology, Mount Sinai Medical Center, New York, New York; ‖Elisabeth Brambilla, CHU Albert Michallon, Institut de Biologie, Département d'Anatomie et Cytologie Pathologiques, Grenoble Cedex, France; ¶Brigham and Women's Hospital, Boston, Massachusetts; #Department of Pathology, Seoul National University College of Medicine, Seoul National University Bundang Hospital, Seongnam, South Korea; **Department of Pathology, University of Pittsburgh, Pittsburgh, Pennsylvania; ††Piedmont Pathology Associates, Hickory, North Carolina, and University of North Carolina, Chapel Hill, North Carolina; ‡‡Department of Medicine and Pathology, University of Colorado Cancer Center, Aurora, Colorado; §§Division of Pathology, The Cancer Institute, Japanese Foundation Cancer Research, Tokyo, Japan; ‖Department of Pathology, Aberdeen Royal Infirmary, Aberdeen, United Kingdom; ¶¶Department of Pathology, CHU A Michallon, INSERM U 823-Institut A Bonniot-University J Fourier, Grenoble, France; ##Department of Pathology, Cancer Center Hospital, Tsukuba, Japan; ***Department of Pathology, Institute of Basic Medical Sciences, University of Tsukuba, Tsukuba, Japan; †††Department of Pathology, Memorial Sloan Kettering Cancer Center, New York, New York; ‡‡‡Department of Pathology and Laboratory Medicine, Fondazione IRCCS Istituto Nazionale Tumori, and Università degli Studi of Milan, Milan, Italy; §§§Institut für Pathologie, Jena, Germany; ‖‖‖Duke University Medical Center, Durham, North Carolina; ¶¶¶University of Texas MD Anderson Cancer Center, Houston, Texas; ###Department of Pathology and Molecular Diagnostics, Aichi Cancer Center, Nagoya, Japan; ****Department of Oncology and Radiotherapy, Medical University of Gdańsk, Gdańsk, Poland; ‡‡‡‡Department of Pathology, University Health Network-Princess Margaret Hospital and University of Toronto, Toronto, Canada; and §§§§Department of Histopathology, Royal Brompton and Harefield Hospitals NHS Foundation Trust and National Heart and Lung Institute, Imperial College, London, United Kingdom.

Disclosure: The authors declare no conflict of interest.

Address for correspondence: Erik Thunnissen, VU Medical Center, De Boelelaan 1117, Amsterdam 1081HV, The Netherlands. E-mail: e.thunnissen@vumc.nl

ISSN: 1556-0864/14/0909-1354

The 2004 World Health Organization (WHO) classification of lung cancer contained three major forms of non–small-cell lung cancer (NSCLC): squamous cell carcinoma (SqCC), adenocarcinoma (AdC), and large cell carcinoma.[1] With an update to the classification of AdC, being published by the International Association for the Study of Lung Cancer/American Thoracic Society/European Respiratory Society containing additional

changes to terminology make the classification more relevant to clinical management and the molecular biology of AdC.[2] Following this, the IASLC pathology committee published a reproducibility study supporting its usage in a routine diagnostic setting[3] and the accuracy in distinguishing better differentiated SqCCs from AdCs has been repeatedly demonstrated elsewhere.[4–7]

However, there are a few data on the reproducibility between pathologists in relation to more poorly differentiated tumors, especially in small biopsies.[8] Specifically, in this setting, the differential diagnosis often lies between a poorly differentiated SqCC and large cell carcinoma, basaloid carcinoma, sarcomatoid or pleomorphic carcinoma, lymphoepithelial-like carcinoma (LELC), and solid AdC. Until recently, there was no clinical imperative for further differentiation, with cases being classified as NSCLC-not otherwise specified (NOS). However, with advances in chemotherapy, there is an increasing need for accurate subdivision, even in these more poorly differentiated neoplasms.[9] Current WHO criteria are purely morphologic for SqCC, these being the presence of keratinization and/or the presence of intercellular bridges, the latter criterion being especially relevant in more poorly differentiated tumors.

Therefore, the goal of this study was first, to assess the reproducibility of a set of histopathological features for SqCC in relation to other poorly differentiated NSCLCs, using a panel of pulmonary pathologists from three continents. Second, we assessed the value of immunohistochemistry (IHC) in improving the diagnosis as an ancillary tool.

MATERIALS AND METHODS

Resection specimens ($n = 80$) with SqCC (well and poorly differentiated), and other cases with diagnosis according to the WHO classification 2004[1] (large cell carcinoma, basaloid carcinoma, sarcomatoid or pleomorphic carcinoma, LELC, and AdC with a solid pattern), were contributed by 10 participating pathologists. Hematoxylin and eosin (H&E)–stained slides were sent to the Tsukuba Critical Path Research and Education Integrated Learning Center at the University of Tsukuba. NanoZoomer 2.0-HT:C9600-13 system was used to scan the slides, Hamamatsu Photonics, Hamamatsu, Japan. The digitized cases were made available on the Internet for reading by the participants.

In this pilot study, 19 histological criteria were considered by the IASLC pathology committee as of possible value in the discrimination of poorly differentiated tumors and, in 80 cases, were scored for their presence, as described in Table 1, with a preferred diagnosis made by 12 pathologists, revealing a low κ score (data not shown).

After this pilot study, the histological criteria were re-evaluated. Six of the criteria were discarded as they were not informative (their presence or absence was not discriminating for any diagnostic category) for the cases, leaving **12 criteria** to be used for further evaluation (printed in **bold** in Table 1). Detailed images were taken from the digitally scanned slides, placed in a Powerpoint file as examples, and consensus definitions of individual histological features were agreed upon (Table 2).

To facilitate the application of the WHO criteria, a flow chart was made, see Figure 1.

TABLE 1. The Criteria Evaluated in the First Round Are Shown and Scored for Each Case as One of the Three Choices

Criterion			
1 Keratinization	Yes	No	Uncertain
2 Pearl formation	Yes	No	Uncertain
3 Intercellular bridges	Yes	No	Uncertain
4 Peripheral palisading of nuclei	Yes	No	Uncertain
5 Intercellular gaps	Yes	No	Uncertain
6 Sheets of polygonal cells	Yes	No	Uncertain
7 Spindle cells	Yes	No	Uncertain
8 Giant cells	Yes	No	Uncertain
9 Pleomorphic cells	Yes	No	Uncertain
10 Cell borders	Rarely seen	In between	Sharp
11 Nuclei	Monomorphic	In between	Pleomorphic
12 Nuclear moulding	Yes	No	Uncertain
13 Chromatin	Finely granular	In between	Vesicular
14 Nucleoli	Inconspicuous	In between	Prominent
15 Glassy eosinophilic cytoplasm	Yes	No	Uncertain
16 Intracytoplasmic vacuoles	Yes	No	Uncertain
17 Mitoses	Low <1/10 HPF = ~0.5 mm	In between	Many >1–2/HPF = ~0.5 mm
18 Mitoses	Absent	In between	Prominent
19 Lymphocytic infiltrate	Absent		
	Present in stroma	Between tumor cells	In both compartments
Comment: [max500 characters]			

In the second round only the bold criteria were scored.
HPF, high power field.

TABLE 2. Definitions for Individual Criteria Formulated after First Ring Study

Intercellular bridges	The gaps that have real bridges are often relatively narrow, are always bordered by cytoplasm, usually plenty of eosinophilic, glassy stuff, and show a constant width. Intercellular bridges are typically seen between elongated cells and are best confirmed at 40× microscope objective (not 20×). The intercellular bridges show several (at least three) connections across the intercellular gap and have a regular quality, similar to the spokes of a wheel or the parallel rungs of a ladder, see Figure 1. In very well-fixed specimens, one may see a tiny dot in the center of the strand between the two adjacent cells, which represents the macula adherens (desmosome), but this is uncommonly seen. Intercellular bridges are a defining criterion for squamous differentiation. They are also prone to overinterpretation, especially when the gaps are not tight and parallel.
Keratin/keratinization	A squamous pearl or a maturing sheet or ball of stratified (± palisading!) epithelium is an easily recognized feature of SqCC. Usually the cytoplasm is glassy, pink, and intercellular bridges are present. The individual cell with keratinization has an intact nucleus with eosinophilic ring around the nucleus and correlate with perinuclear tonofibrillar bundles ultrastructurally. This may be tricky and prone to over interpretation, i.e., pyknotic nuclei with dense eosinophilic cytoplasm cannot be used for identification of individual cell keratinization. Individual cell death (apoptosis) can be falsely interpreted as keratinization. Individual cell keratinization is beside pearl formation and intercellular bridges also defining for squamous differentiation.
Intercellular gaps	Intercellular gaps are quite a common finding in many lung cancers, which is mostly an artifact, representing fixation and processing changes. It is a change which is often misinterpreted as indicating squamous differentiation, probably because gaps are needed to see bridges and so, pathologists can "see"—maybe actually imagine—bridges when gaps are present. Image 2 show lots of gaps where there are no intercellular bridges and the impression is that the gaps without bridges are wide, uneven, and variable. Sometimes there is little or no cytoplasm apparent between the nucleus and the gap. Intercellular gaps are not diagnostic for squamous cell or other carcinomas.
Intracytoplasmic vacuoles	Vacuoles are according to Stedman's Medical Dictionary, defined as a "clear space in the substance of a cell, sometimes degenerative in nature." Vacuoles may hint at the possibility of an adenocarcinoma but never define or confirm the diagnosis—and may be seen in all sorts of tumors as degenerative changes. Vacuoles might trigger a mucin stain—the mucin stain may confirm adenocarcinoma differentiation. For the purpose of this study with intracytoplasmic vacuoles those vacuoles are meant, which may have a high chance to be positive in the mucin stain, see Figure 3. Vacuoles can be round, oval or odd shapes and their location in the cell is not of much help. Mucin stain is less likely to be positive if there were multiple vacuoles and just beneath the cell membrane and more likely to be positive if single, big and look as if they had something in them. In essence vacuoles are frequently seen in any carcinoma, but those which are more frequently associated with mucin positivity open the possibility of adenocarcinoma (solid type).
Palisading	Palisading is defined as layer of relatively long cells with nuclei arranged loosely perpendicular to a surface and parallel to each other. Palisading is not a defining feature of SqCC and is seen in other tumors (i.e., basaloid carcinoma, adenocarcinomas and neuroendocrine carcinomas). However, in the correct context, it might be useful to raise the possibility of SqCC, assuming other features are present. There was no consensus on what was exactly meant with this feature, Figure 4.
Lymphocytic infiltrate	Lymphocytes occur regularly in stroma of NSCLC. In LELC, an appreciable number of intratumoral lymphocytes are present: i.e., in the nest between tumor cells, Figure 5. Small numbers get ignored. In Eastern countries, EBV is usually positive, but in Western countries usually negative. The LELC may become defined by the presence of EBV. For the purpose of this study, the presence and location of the lymphocytes were recorded.
Sheets of polygonal cells	Sheets or nests of polygonal cells are a characteristic of epithelial architecture, see Figure 1. In case of a malignant tumor, it is pointing toward a carcinoma instead of sarcoma or lymphoma. "Sheets of polygonal cells" is thus not restricted to SqCC. In larger areas of sarcomatoid carcinoma, sheets are usually lacking.
Spindle cells	According to the WHO 2004, a spindle cell carcinoma "consists of only spindle-shaped cells," architecturally nests/fascicles with overtly malignant nuclear features (Fig. 6). As for calling, a case sarcomatoid carcinoma unanimous consensus was present in case of diffuse mesenchymal spindle appearance of the tumor, this pattern was used for designation of "spindle." Whereas with some spindle-like cells in more nested tumors (mixed with epitheloid nuclei), the variation was much larger.
Glassy eosinophilic cytoplasm	Is an eosinophilic cytoplasm, which is not unique to SqCC carcinoma, but is frequently present when defining criteria for SqCC were also present. Eosinophilic cytoplasm may also occur in adenocarcinomas, especially in invasive areas.
Giant cells	No consensus
Nuclear moulding	Nuclear moulding is a frequent finding in small-cell lung carcinoma, but a rare feature in SqCCs. However, it may occasionally be present in small-cell type SqCC.

SqCC, squamous cell carcinoma; NSCLC, non–small-cell lung cancer; LELC, lymphoepithelial-like carcinoma; WHO, World Health Organization.

To assess the reproducibility of diagnosis in poorly differentiated tumors, a ring study was performed in which 37 of the initial 80 digitized cases were read in a second ring study by 16 pathologists. The reduction to 37 cases was based on the information from the pilot study that κ scores did not essentially change by reading more cases. The interval between the pilot study and this ring study was 12 months.

In contrast to the pilot study, two levels of diagnosis were evaluated. First, the (differential) diagnosis on H&E alone was scored. Subsequently, the immunohistochemical information (i.e., the result from the submitting pathologist regarding TTF1, mucin, and p63/p40) was provided, allowing the pathologist to make a "second level" integrated diagnosis based on H&E plus additional stains, should they wish.

Statistics

The distribution of the readers' diagnoses was compared with the original submitting pathologist's diagnosis. The κ scores were calculated in two different ways: (1) between all diagnostic categories for all possible combinations of pathologists and diagnostic categories and (2) for each individual diagnostic category versus all the other diagnostic categories combined. For each pathologist, the sensitivity and specificity of the score, for

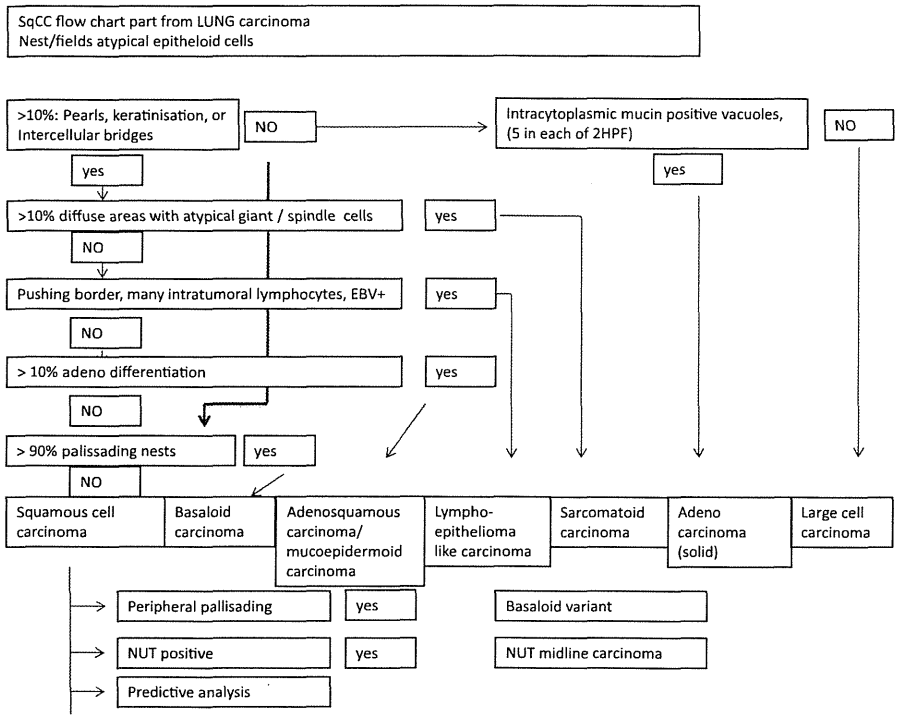

FIGURE 1. A flow chart for the application of histological criteria in poorly differentiated SqCC based on the WHO classification 2004.[1] HPF, high power field; NUT, *NUT* midline carcinoma, family member 1 (*NUTM1*); SqCC, squamous cell carcinoma; WHO, World Health Organization.

example, SqCC (criteria 1–3 in Table 1 with at least one "yes") and for p63/40 positivity was computed, as well as Youden's J statistic (the sum of the sensitivity and specificity minus 1). The same was undertaken for the sensitivity, specificity, and Youden's J statistic for a positive score for intracytoplasmic vacuoles ("yes") and for thyroid transcription factor/mucin positivity. Associations between the two categorical variables were tested by the χ^2 test.

For statistical analysis, the SPSS software package version 20.0 (IBM Corp., Armonk, NY) was used.

RESULTS

Descriptions of Histological Criteria

Detailed descriptions for the interpretation of histological criteria were made (Table 2 and Figs. 2–7). To assess the reproducibility of poorly differentiated NSCLC, 16 pathologists read 37 cases. The original contributors' diagnoses were SqCC (n = 13), basaloid carcinoma (n = 5), AdC solid type (n = 4), large cell carcinoma (n = 6), sarcomatoid carcinoma (n = 5), and LELC (n = 4).

In nine cases, the presence of "keratinization" was scored by a majority of pathologists (mean, 83%; range, 62–94%), while in the other 28 cases, on an average, one pathologist (mean, 4%; range, 0–25%) scored "keratinization" as being present. In six of these first nine cases, "pearl formation" was also scored as being present by the majority of the pathologists (mean, 63%; range, 25–88%). "Intercellular bridges" were also seen in seven of these nine cases by the majority (mean, 74%; range, 25–94%), while these features were rarely scored in the other 26 cases. Thus, only a minority of the 37 cases consisted of SqCC according to the readers. "Intercellular gaps" were scored as being present slightly more often in the cases with keratinization, as compared to the others, suggesting that this feature is not specific for this differential diagnosis.

To establish consistency in the use of the histological criteria, the relation between scored histological criteria and specific diagnosis provided by the same observer is shown in Table 3. In general, the three squamous cell criteria (keratinization, squamous pearls, and intercellular bridges) were scored present in 17 to 25% of all the scores (n = 592: 16 pathologists × 37 cases). These three criteria were highly correlated (r > 0.50, data not shown) and mainly distributed over SqCC and sarcomatoid carcinoma. In these sarcomatoid carcinomas, an area of SqCC was present according to the original diagnosis.

"Sheets of polygonal cells" and "intercellular gaps" were scored as present in 85% and 58%, respectively, scored in all diagnostic categories, but mainly distributed over SqCC and large cell carcinoma. "Peripheral palisading of the nuclei," "glassy eosinophilic cytoplasm," "spindle cells," and "giant cells" were scored in SqCC and large cell carcinoma. "Glassy eosinophilic cytoplasm" and "spindle cells" were also scored in sarcomatoid carcinoma. "Giant cells" were frequently scored in sarcomatoid carcinoma. "Nuclear moulding" was rarely scored (12%), but when present, was seen in SqCC, basaloid, and large cell carcinoma. Lymphocytes in stroma were present in 80% of the scores, and lymphocytes admixed amongst the tumor cells in 35%. The score for "intracytoplasmic vacuoles" was 22%, distributed over large cell carcinoma, SqCC, and AdC.

Additional Stains and Criteria

In cases with submitted diagnosis of SqCC, additional stains for AdC differentiation (TTF1/mucin) and p63/40 were

TABLE 3. The Histologic Criteria Scored to Be Present (*n*/% of Positive Scores) for the Diagnosis of the Same Observer Is Shown, Plus Sum of These Scores and % of Total Scores (Total = 592)

Diagnosis	SqCC	Basaloid	AdC	Ad.SqC	LCC	Sarc.	LELC	Total	% Total
Keratinization	109	2	0	1	5	21	0	138	23%
	79%	1%	0%	1%	4%	15%	0%		
Pearl formation	74	2	0	1	4	18	0	99	17%
	75%	2%	0%	1%	4%	18%	0%		
Intercellular bridges	122	1	0	0	5	20	0	148	25%
	82%	1%	0%	0%	3%	14%	0%		
Intercellular gaps	140	14	16	1	130	34	6	341	58%
	41%	4%	5%	0%	38%	10%	2%		
Peripheral palisading nuclei	67	24	6	0	51	6	0	154	26%
	44%	16%	4%	0%	33%	4%	0%		
LI between tumor cells	3	0	3	0	13	3	3	25	4%
	12%	0%	12%	0%	52%	12%	12%		
LI in stroma	116	21	14	1	127	15	0	294	49%
	39%	7%	5%	1%	43%	5%			
LI in both compartments	40	3	12	1	93	14	22	185	31%
	22%	2%	6%	1%	50%	8%	12%		
Sheets polygonal cells	152	22	27	2	244	39	19	505	85%
	30%	4%	5%	0%	48%	8%	4%		
Spindle cells	35	3	6	1	39	43	0	127	21%
	28%	2%	5%	1%	31%	34%	0%		
Giant cells	32	0	4	0	30	23	0	89	15%
	36%	0%	4%	0%	34%	26%	0%		
Glassy eosinophilic cytoplasm	112	3	7	2	83	27	2	236	40%
	47%	1%	3%	1%	35%	11%	1%		
Intracytoplasmic vacuoles	23	0	18	1	75	10	1	128	22%
	18%	0%	14%	1%	59%	8%	1%		
Nuclear moulding	10	16	2	1	40	2	0	71	12%
	14%	23%	3%	1%	56%	3%	0%		

SqCC, squamous cell carcinoma; Basaloid, basaloid carcinoma; AdC, adenocarcinoma; Ad.SqC, adenosquamous carcinoma; LCC, large cell carcinoma; Sarc, sarcomatoid carcinoma; LELC, lymphoepithelial-like carcinoma; LI, lymphocytes.

requested in 73% and 78% of the cases, respectively. For the other diagnoses, this fraction was higher with 91 and 92%, respectively, indicating the relatively undifferentiated morphology of these latter cases, as well as, the wish for immunohistochemical information in these cases.

In Table 4, the relation between the scored histological criteria and additional stains for AdC (TTF1 and mucin) and SqCC is shown. In general, the squamous cell criteria are usually scored as present in cases positive for p63/p40, and not scored as present when AdC stains were positive (for all $p < 0.001$). A similar finding was shown for palisading of the nuclei. Intracytoplasmic vacuoles scored as present were more frequently associated with positive AdC differentiation stains and less frequently with positive p63/p40. The remaining criteria did not show a significant relation with these additional stains.

Observer's Diagnosis Compared to Diagnosis of Submitting Pathologist

The distribution of original diagnosis from submitting pathologist compared to diagnosis of 16 pathologists is shown for two different levels in Table 5. The first level is based on hematoxylin and eosin (H&E) only and the second level on H&E combined with information from the additional stains: p63/p40, TTF1, and/or mucin. The overall κ score (95% confidence interval [CI]) at the first level was 0.31 (eight categories, 95% CI, 0.23–0.40), and increased to 0.45 (seven categories, 95% CI, 0.37–0.53) at the second level, showing an essential improvement with the use of additional stains.

Reproducibility of Diagnostic Categories

In Table 6, the κ scores for each individual diagnostic category versus all other categories combined are shown. For most individual categories, the κ score improved (or remained above 0.46) with the use of additional stains, in the case of SqCC, solid AdC, sarcomatoid carcinoma, and LELC. For basaloid carcinoma, adenosquamous carcinoma, and large cell carcinoma, the κ score remained below 0.30 after the use of additional stains.

Interobserver Variation Criteria Related to Additional Stains

For each pathologist, the relation between the presence of H&E features of squamous differentiation and p63/40 was

TABLE 4. Relation between a Score of "Yes" for Individual Criteria (*n* and %) and TTF1 (Total Scores *n* = 576) and p63/p40 (Total Scores = 560)

	TTF1 and/or Mucin					p63/p40				
	Negative		Positive			Negative		Positive		
Criterion	***n***	**%**	***n***	**%**	***p* Value**	***n***	**%**	***n***	**%**	***p* Value**
Keratinization	132	29%	6	5%	<0.001	2	2%	134	31%	<0.001
Pearl formation	94	21%	5	4%	<0.001	1	1%	97	22%	<0.001
Intercellular bridges	139	31%	9	7%	<0.001	7	5%	139	32%	<0.001
Intercellular gaps	284	63%	61	48%	0.001	81	63%	254	59%	0.36
Peripheral palisading of nuclei	136	30%	21	16%	0.002	20	16%	136	31%	<0.001
Sheets polygonal cells	392	88%	110	86%	0.64	109	85%	379	88%	0.44
Spindle cells	95	21%	32	25%	0.36	32	25%	80	19%	0.11
Giant cells	74	17%	16	13%	0.27	23	18%	60	14%	0.25
Glassy eosinophilic cytoplasm	185	41%	58	45%	0.42	59	46%	180	42%	0.37
Intracytoplasmic vacuoles	78	17%	42	33%	<0.001	36	28%	79	18%	0.02
Nuclear moulding	63	14%	9	7%	0.03	16	13%	55	13%	0.94

TABLE 5. The Original Diagnosis of Submitting Pathologist Is Compared to Diagnosis (in %) of 16 Pathologists Based on H&E only and Including Information Additional Stains (p63/p40, TTF1, Mucin)

		Original Diagnosis					
		SqCC	**Basal**	**Adeno**	**LCC**	**Sarcom.**	**LELC**
	Diagnosis	**%**	**%**	**%**	**%**	**%**	**%**
H&E only	SqCC	59%	11%	9%	11%	20%	9%
	Basaloid	2%	24%	0%	7%	0%	0%
	AdC	0%	1%	33%	6%	5%	3%
	AdenoSqmC	0%	1%	2%	0%	0%	0%
	LCC	33%	55%	52%	65%	28%	56%
	Sarcom.	2%	1%	0%	5%	48%	0%
	LELC	2%	0%	2%	2%	0%	28%
	DD SqCC-AdC	2%	6%	3%	3%	0%	3%
	Total	100%	100%	100%	100%	100%	100%
H&E plus stains	SqCC	76%	31%	3%	19%	13%	14%
	Basaloid	4%	33%	0%	14%	0%	0%
	AdC	0%	1%	70%	8%	10%	8%
	AdenoSqmC	0%	6%	2%	1%	0%	2%
	LCC-Sqcc	10%	19%	3%	19%	1%	14%
	LCC-AdC	0%	1%	11%	7%	9%	5%
	LCC-AdenoSqmC	0%	3%	8%	2%	3%	0%
	LCC-undiff	4%	6%	2%	22%	5%	28%
	Sarcom.	2%	0%	0%	6%	60%	0%
	LELC	3%	0%	2%	2%	0%	30%
	Total	100%	100%	100%	100%	100%	100%

SqCC, squamous cell carcinoma; Basaloid, basaloid carcinoma; AdC, adenocarcinoma; AdenoSqmC, adenosquamous carcinoma; LCC, large cell carcinoma; Sarcom., sarcomatoid carcinoma; LELC, lymphoepithelial-like carcinoma; DD SqCC-AdC, combination of SqCC and adenocarcinomas in the differential diagnosis; LCC-SqCC, large cell carcinoma favor SqCC; LCC-AdC, large cell carcinoma favor adenocarcinoma, LCC-Adenosquameus carcinoma; LCC-undiff, large cell carcinoma, additional stains negative.

similar: the mean and SD of the observers' sum of sensitivity and specificity were 133±13%. The ideal maximum is the sum of 100% sensitivity and 100% specificity = 200%. For the presence of intracytoplasmic vacuoles and TTF1/mucin positivity, these values were 115±17%. These data emphasize that more information about differentiation is obtained in undifferentiated or poorly differentiated tumors with the use of additional stains, than is recognized by light microscopic criteria alone in H&E-stained slides.

TABLE 6. Kappa Score (Two Categories: Specific Category vs. the Others; 95% Confidence Interval in Brackets) for Diagnostic Categories Based on (1) H&E Diagnosis Alone and on (2) Stains: Diagnosis Including Information Additional Stains (p63/p40, TTf1, Mucin)

	SqCC	Basaloid	AdC	AdenoSqmC	LCC	Sarcom.	LELC
H&E	0.46 (0.33–0.59)	0.27 (0.19–0.36)	0.21 (0.10–0.33)	0.05 (0.0–0.19)	0.25 (0.15–0.36)	0.52 (0.35–0.69)	0.56 (0.36–0.76)
H&E + stains	0.46 (0.33–0.59)	0.25 (0.16–0.34)	0.53 (0.33–0.73)	0.09 (0.0–0.19)	Range[a] (0.12–0.21)	0.52 (0.34–0.69)	0.47 (0.34–0.60)
Combining categories							
H&E	0.36 (0.25–0.48)		0.21 (0.10–0.33)	0.05 (0.0–0.10)	0.25 (0.15–0.36)	0.52 (0.35–0.69)	0.56 (0.36–0.76)
H&E + stains	0.57 (0.45–0.70)		0.63 (0.46–0.81)	0.20 (0.10–0.29)	0.21 (0.04–0.38)	0.52 (0.34–0.69)	0.47 (0.34–0.60)

After combining two diagnostic categories κ scores were recalculated. For this SqCC and basaloid was defined as one category; large cell carcinoma favoring SqCC was combined with SqCC; large cell carcinoma, favoring AdC with adenocarcinoma; large cell carcinoma, favoring AdenoSqmC to AdenoSqCC. Large cell carcinoma, unclassified after stains remained the large cell category.

SqCC, squamous cell carcinoma; Basaloid, basaloid carcinoma; AdC, adenocarcinoma; AdenoSqmC, adenosquamous carcinoma; LCC, large cell carcinoma; Sarcom., sarcomatoid carcinoma; LELC, lymphoepithelial like carcinoma.

[a]Range for the following categories: large cell carcinoma, favoring SqCC; large cell carcinoma, favoring AdenoC; large cell carcinoma, favoring AdenoSqCC; large cell carcinoma, unclassified.

DISCUSSION

Histologic criteria are consistently used by pathologists according to WHO criteria[1], but in poorly differentiated cases of NCSLC, many may not be present and the definitions are subject to individual interpretation, rendering consistent diagnosis more difficult and raising the possibility of a range of differential diagnoses based on cytological pleomorphism rather than aspects of differentiation. Also, this study demonstrates that, with the use of ancillary stains in poorly differentiated NSCLC, improved reproducibility can be obtained for the histopathological categories SqCC, solid AdC, sarcomatoid carcinoma, and LELC. Furthermore, it highlights the need for more precise definitions of individual histologic criteria, something evidenced in earlier studies relating to the definition of invasion.[3]

In relation to ancillary stains, the reproducibility between pathologists in poorly differentiated lung cancer has been shown to be poor in the past,[10,11] indicating that in H&E stained sections, diagnostic criteria are harder to find and may increase the likelihood of diagnosis of large cell carcinoma in resection specimens. There are numerous publications showing that the addition of IHC reduces the NOS rate in biopsy and also may potentially reclassify the number of cases termed LCC,[12–17] but our data additionally suggest that applying the current criteria and practice would lead to higher κ values in daily practice than on H&E alone, especially in these more poorly differentiated tumors.[7]

However, it is important to realize that these additional staining criteria do not have a defining capacity by themselves, as these stains are neither 100% specific nor sensitive. p63 may stain some AdCs, and TTF1 has a sensitivity of 70 to 80% in AdCs, plus both antibodies may stain tumors from other sites. Nevertheless, in the context of tumors where classification comes down to the differential of more poorly differentiated NSCLCs, these stains provide ancillary data that improve the accuracy of pathological diagnosis.

The consistent use of histological criteria is essential for histopathological diagnosis. In our study, the first phases of the study uncovered variations in interpretation of the individual criteria and we, therefore, made slightly stricter definitions (Table 2) even though some of the defining SqCC criteria (keratinization, squamous pearls, and intercellular bridges) originated 5 decades ago.[18] Again, this highlights the importance of ensuring that the written definitions are open to as little variation in interpretation as possible.

Even with stricter definitions, some criteria were found to be problematic in relation to the distinction of SqCCs from other subgroups. These included the term "intercellular gaps," which some pathologists were misinterpreting as the "intercellular bridges" of true squamous differentiation. Furthermore, "glassy eosinophilic cytoplasm" may also be recognized in AdCs and large cell carcinomas with mucin or TTF1 positivity and may reflect what some have termed "pseudo-squamoid" morphology.[19] Neither of these criteria appear to be of value in histologic distinction on H&E staining. Furthermore, the architectural terms "sheets of cells" may have a limited descriptive value in the distinction of epithelioid tumors from sarcomatoid tumors, but otherwise has little diagnostic value in the subtyping of NSCLCs.

Conversely, cytological criteria such as "spindle cells" in the context of a diffuse pattern with fascicles reached consensus and were of value in the classification of sarcomatoid carcinomas, although they were described in cases classified by some as SqCC. This, therefore, highlights the importance in documenting evidence of both squamoid and AdC differentiation in these more poorly differentiated epithelial tumors that are showing increased cellular plasticity. Moreover, the presence of sarcomatoid areas in greater than10% renders the diagnosis of sarcomatoid carcinoma and trumps squamous cell or AdC (Fig. 1).[1]

Despite some histological criteria being shown to have diagnostic value in more poorly differentiated tumors, our study shows that there is considerable overlap in these features that are helpful, for recognition of certain subtypes and are also discerned in the others. The examples are: features such as "intracytoplasmic vacuoles" which were scored as being present in cases finally classified as both SqCC and large cell carcinoma. Some of these may reflect a lack of mucin stains. Recently, the presence of two mucin droplets, instead of five in two high power fields was shown to be sufficient for diagnosis of AdC.[8] Moreover, recognition of these features is also dependent on having a good quality, well stained section of the correct thickness to examine.